

# 1st CEPHONA Workshop on Microscopic Characterisation of Materials and Structures for Photonics

Warsaw, November 24, 2003

## ELECTRON MICROSCOPY OF ADVANCED OPTOELECTRONIC STRUCTURES

Jerzy KAŹCKI

*Institute of Electron Technology, Al. Lotników 32/46, 02-668 Warsaw, Poland*

### ABSTRACT

The most important application of cross-sectional transmission electron microscopy (TEM) and scanning electron microscopy to the investigation of optoelectronic devices are reviewed. A technique of TEM specimen preparation was introduced. Special attention was paid to the electron microscopy assessment of the growth perfection of such crucial elements of the devices like quantum wells, quantum dots, distributed Bragg reflectors as well as electrical contacts. Using these examples the most important issues of the application of electron microscopy to characterization of optoelectronic devices are discussed.

### 1. INTRODUCTION

Electron microscopy is a very useful technique for assessing the quality of heterostructures both at the final stage of the epitaxial growth as well as at the various stages of device processing. Especially useful for the characterization of advanced optoelectronic heterostructures is cross-sectional transmission electron microscopy (XTEM). In some cases plan-view TEM observations are also applied.

#### 1. TEM SPECIMEN PREPARATION

In order to observe the crystallographic perfection of a semiconductor heterostructure in a transmission electron microscope a thin foil from this material should be prepared. In the past thin foils for TEM study were prepared only in a plane parallel to the wafer surface (Fig. 1). Micrographs obtained in this way were called „*plan-view*” TEM micrographs. This method is very useful when the planar distribution of defects in a single layer is to be analyzed (see quantum dots distributions). In this case other layers are removed by mechanical polishing or selective chemical etching. This method can be also useful when an area of the interface between two layers is to be analyzed.

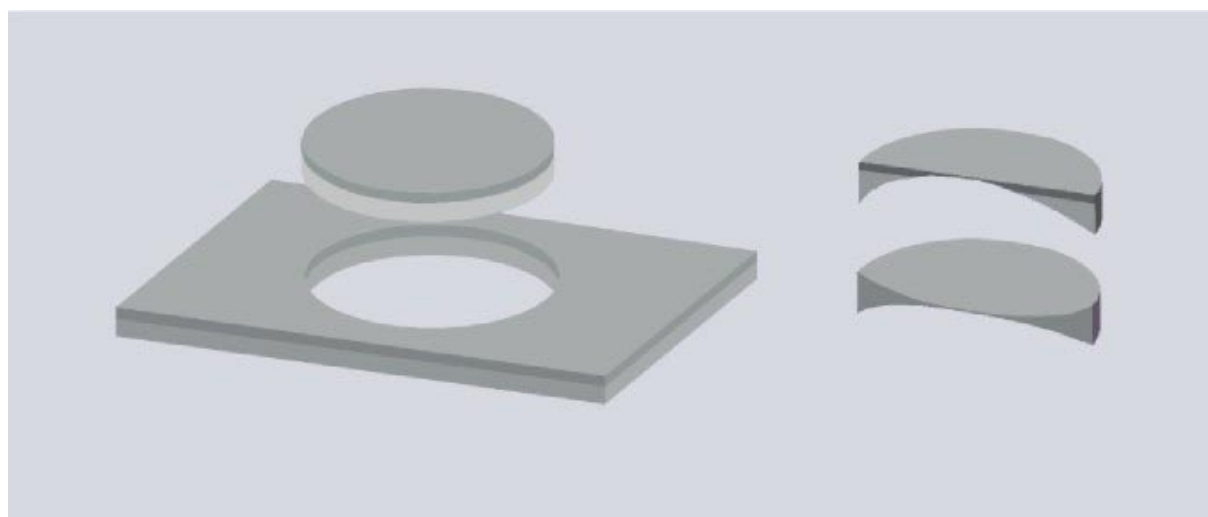


Fig. 1. Plan-view TEM specimen preparation

However, in most cases, a heterostructure consists of many layers and important questions are how perfect the geometry of a heterostructure is and what happens at or near the interfaces. That is why, the most informative micrographs should have all the layers and interfaces together on a single image. Therefore, in many TEM laboratories dealing with semiconductor heterostructures most thin foils from heterostructures are prepared perpendicularly to their surface. Micrographs obtained from such prepared specimens are called „*TEM cross-sections*” [1,2]. In our laboratory we developed an original method for preparing TEM cross-sections allowing us to obtain many specimens from a small piece of the wafer (Fig. 2) [3,4]. We applied this method to prepare all the cross-sectional specimens discussed in this paper.

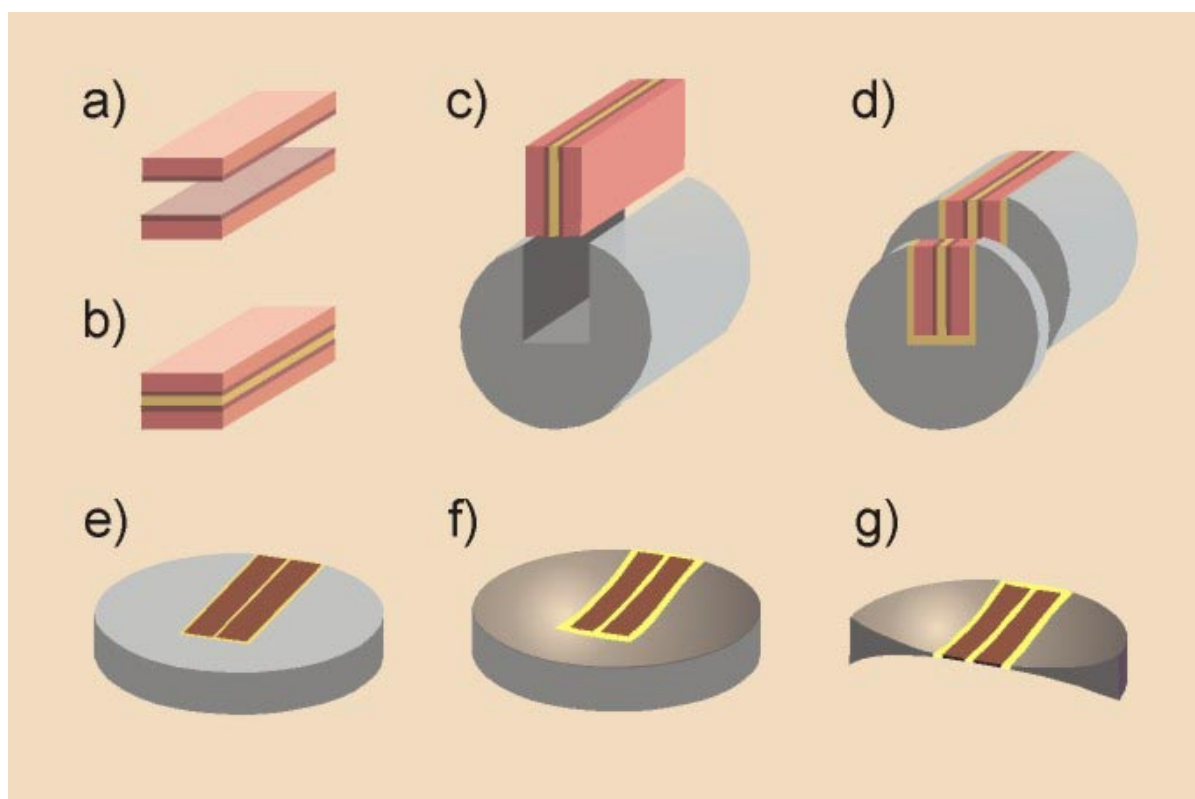


Fig. 2. TEM cross-section preparation

### 3. ELECTRON MICROSCOPY OF LASER STRUCTURES

In a typical VCSEL structure the cavity with a single or multiple (In)GaAs quantum wells is located in between the GaAs/(Ga)AlAs DBRs. The device structure is formed by etching and subsequent metallization (see Fig. 3). In this case SEM images provide a convenient way of visualisation of the whole structure and help to detect technological problems connected with proper controlling of the etching process. The image brings information about uniform distribution of GaAs and AlAs layers, however the measurement of the thickness of subsequent layers is difficult.

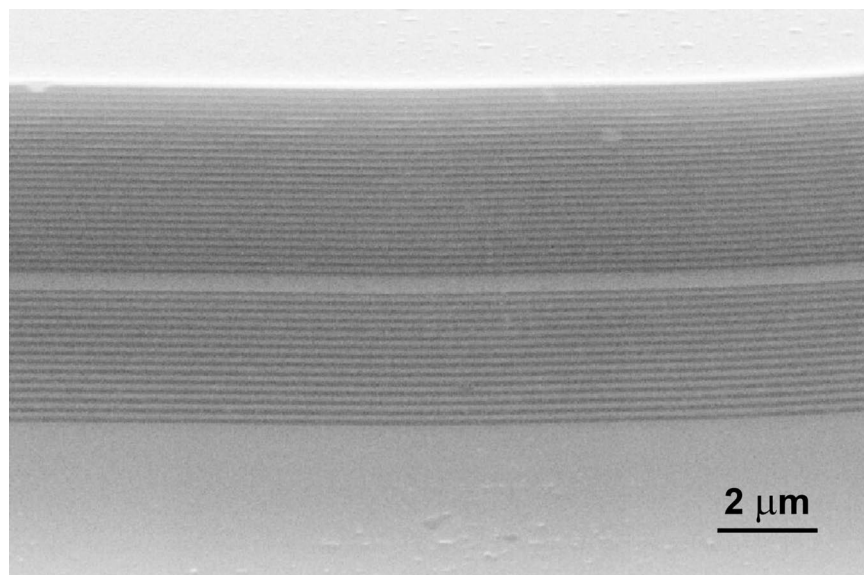


Fig. 3. SEM image of an etched VCSEL structure [5]

#### 3.1. Quantum Wells

The most important part of lasers and light emitting diodes (LEDs) is an active region. The active region of the laser consists of  $\lambda$ -type resonant cavity with either one or three InGaAs QWs, each 8 nm thick separated by 10 nm thick GaAs barriers. They are located in the central part of the  $\lambda$ -thick cavity. Cross-sectional TEM views of an active region with a single and multiple QWs is shown in Figs. 4a and b, respectively. In advanced structures like QDs lasers, a continuous InGaAs QW layer is replaced with QDs layer placed in the middle of the resonant cavity.

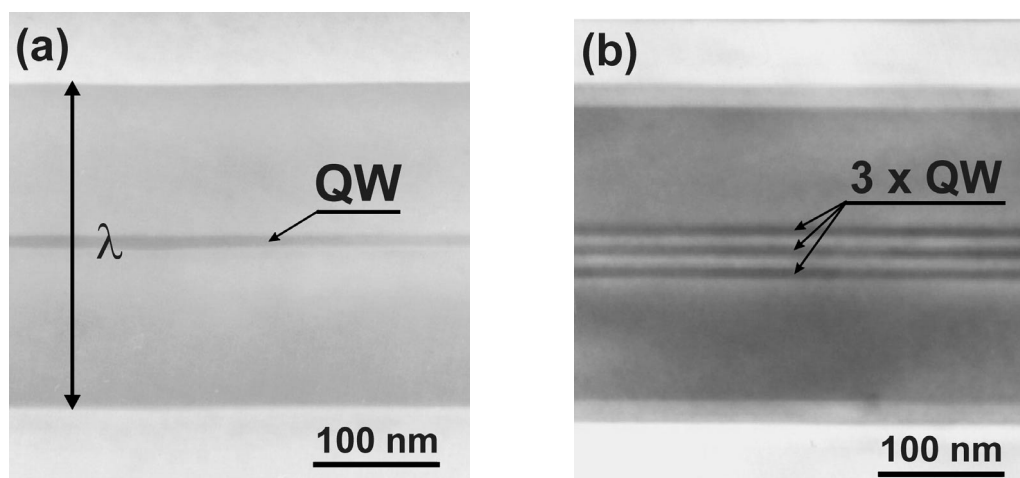


Fig. 4. Cross-sectional views of an active region with (a) single and (b) multiple QWs [5]

### 3.2. Electrical Contacts

For proper operation of devices they must be contacted to allow current flow through the structure. In RCLED structures, typically the Au contact is evaporated at the top of the heterostructure. A cross-sectional view of the contact area can be seen in Fig. 5. In the centre of the image an oxide isolation is visible. The contact itself is visible on the left side of the picture.

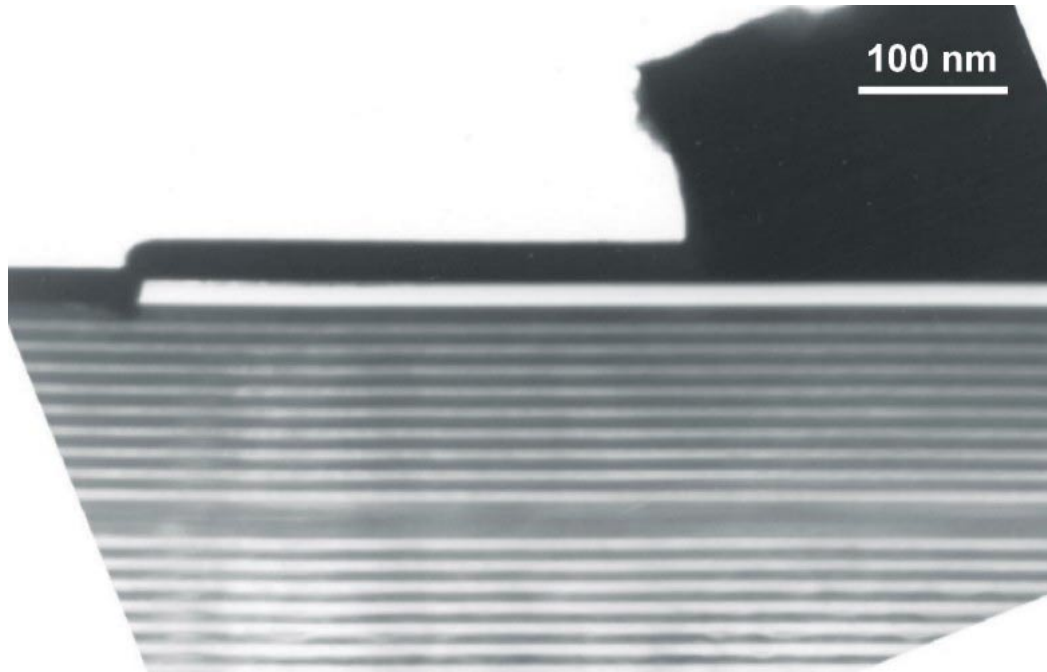


Fig. 5. SEM image of an etched VCSEL structure [5]

Another example of contact structure is shown in Fig. 6a. The cross-sectional TEM view of the Au/ZrB<sub>2</sub>/Ag(Te) contact to GaSb annealed at 250°C for 180 s is presented here. Below the Ag(Te)/GaSb interface dissolution pits were formed. A lattice image of the interface between the dissolution pits (DP) and the GaSb substrate is shown in Fig. 6b. Between the dissolution pits and the GaSb matrix a transition region can be observed.

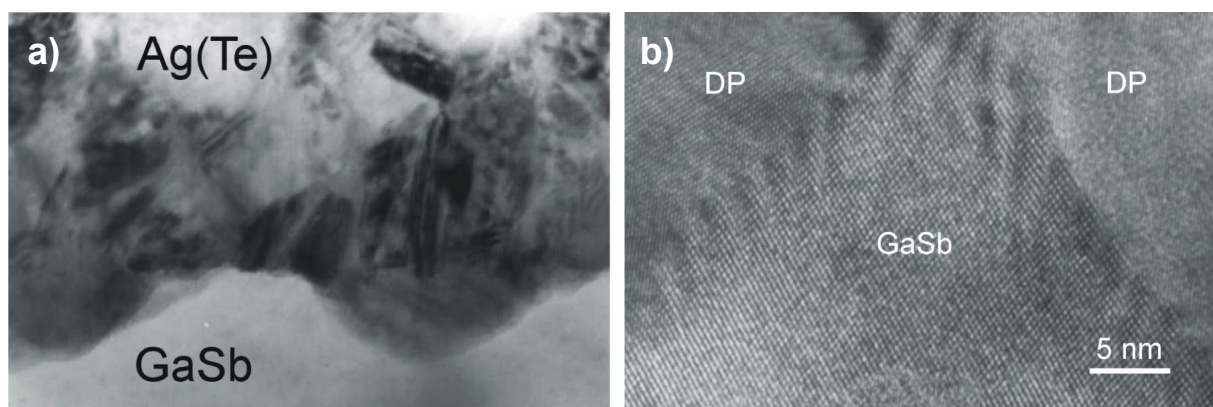


Fig. 6. TEM analysis of the Au/ZrB<sub>2</sub>/Ag(Te) contact to GaSb annealed at 250°C: (a) Ag(Te)/GaSb interface (BF) b) lattice image of the interface between dissolution pits and a GaSb substrate. [6]

### 3.3. Distributed Bragg Reflectors

In Fig. 7 cross-sectional TEM micrographs of two types of DBR interfaces are shown. A DBR with an abrupt GaAs/AlAs interface is presented in Fig. 7a, where GaAs and AlAs layers are visible as dark and bright stripes, respectively. In the DBR shown in Fig. 7b 20 nm thick  $\text{Al}_{0.5}\text{Ga}_{0.5}\text{As}$  layers were added between the GaAs and AlAs layers. These layers are visible as grey stripes. The micrograph is the evidence that the grey level of  $\text{Al}_x\text{Ga}_{1-x}\text{As}$  layers depends on the Al content in  $\text{Al}_x\text{Ga}_{1-x}\text{As}$  alloy. The higher the content of aluminium the brighter the contrast of a layer. A GaAs layer being an example of 0% Al content alloy ( $x=0$ ) looks the darkest. Finally, an AlAs layer is an example of  $\text{Al}_x\text{Ga}_{1-x}\text{As}$  alloy containing 100 % Al ( $x=1$ ). Figure 7c shows a lattice image of the abrupt GaAs/AlAs interface. From the image one can conclude that the interface is smooth and free of defects. In the lattice image the difference in brightness of the contrast of the layers is not so pronounced because in order to obtain a multi-beam images the aperture of large diameter is used. Using the larger diameter aperture ensures that less electrons are scattered outside of the aperture.

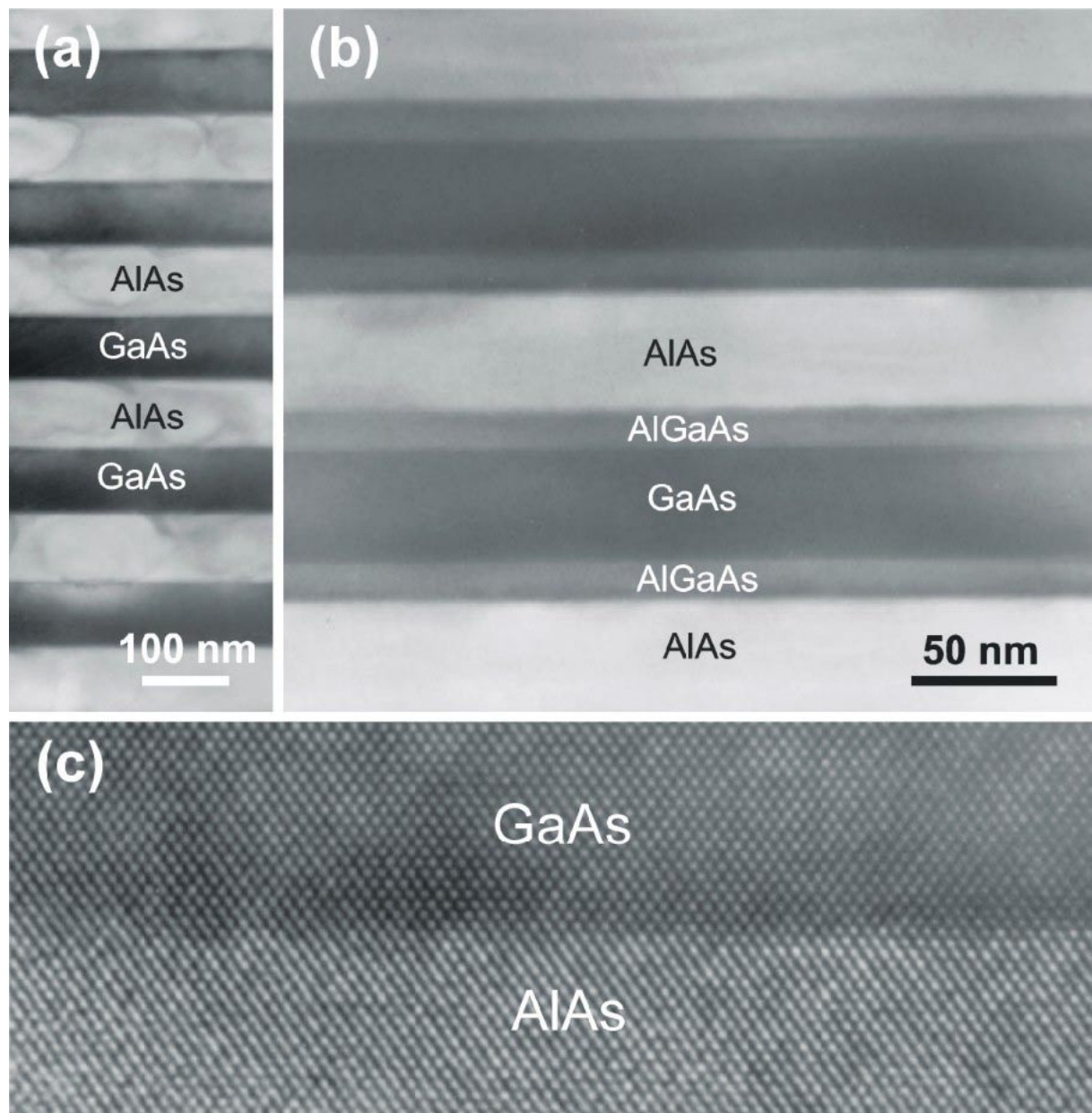


Fig. 7. Cross-sectional TEM views of two types of DBR interfaces: (a) GaAs/AlAs, (b) GaAs/ $\text{Al}_{0.5}\text{Ga}_{0.5}\text{As}$ , and (c) a lattice image of the GaAs/AlAs interface

### 3.4. Quantum dots

Under the Stransky-Krastanov growth mode the formation of QDs is driven by the strain during epitaxial growth of In(Ga)As on the GaAs substrate as the deposited layer exceeds a critical thickness. Then, the growth mode changes from a two-dimensional growth to a three-dimensional growth and the strain is relieved elastically without formation of lattice defects.

In a real structure subsequent layers are deposited on the QD layer and QDs are embedded in a matrix, In QD structures studied in our project quantum dots are typically located 100 - 200 nm below the structure surface.

In Fig. 8a a schematic drawing of a MBE grown QD sample (EPFL) is presented [7]. A cross-sectional TEM image of this sample is shown in Fig. 8b. On this image GaAs and AlAs layers can be easily distinguished since the contrast from AlAs layers is brighter than from layers of GaAs. The exact thicknesses of AlAs and GaAs layers measured from the TEM image are 19 nm and 100 nm respectively. A layer of InAs QDs is located between two GaAs layers. It is covered by a 5 nm thick  $\text{In}_{0.154}\text{Ga}_{0.846}\text{As}$  capping layer. In case of this sample QDs were grown directly on GaAs. Bright contrast from QDs is surrounded by dark contrast from strain formed in the matrix around the dots (especially above and below the dots). The width of the QDs taken from the image is about 20 nm.

Figure 8c shows a TEM plan-view image of the QD sample. In the sample being studied the QDs are located approximately 140 nm below the structure surface. Such a specimen requires thinning only from the back-side. The strain contrast around the dots is easily distinguishable. It is visible as dark symmetrical shapes. The areal density of QDs can be determined by counting the number of QDs in a certain square area. For this sample the areal density of QDs is  $302 \text{ dots}/\mu\text{m}^2$ . From the TEM cross-section the linear density of QDs can be measured. In case of significant amount of dots this density is proportional to the areal density of dots.

We can assume that the thickness of a thin foil constituting a cross-section of the QD structure is below 50 nm. In order to better understand what we see in the cross-sectional image, on the plan-view image shown in Fig. 8c we can imagine two parallel lines, one 50 nm away from another. Dots located in the area between these two lines are visible in Fig. 8b. Since, as we found, the distribution of QDs is uniform and the QD density is high enough, without being mistaken we can say that a cross-sectional sample should contain in its bulk many full-sized QDs.

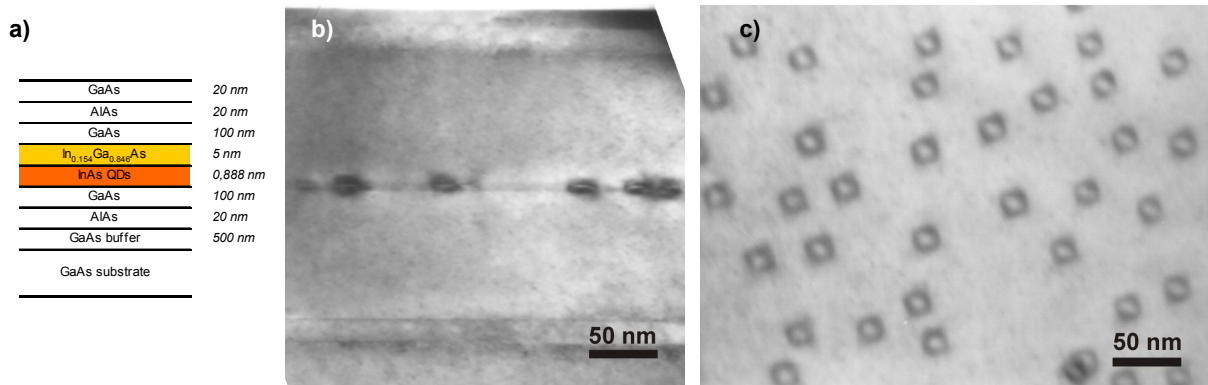


Fig. 8. Analysis of QDs in a TEM: a) schematic drawing; b) cross-sectional image; c) plan-view image. [7]

In Fig. 9a a  $\langle 110 \rangle$ -type lattice image of a MOCVD grown QD is shown. QDs in this sample were grown by deposition of 4ML InGaAs layer on a 3 nm thick  $\text{In}_{0.05}\text{Ga}_{0.95}\text{As}$  layer and capped by a 5 nm thick  $\text{In}_{0.05}\text{Ga}_{0.95}\text{As}$  capping layer [7]. In Fig. 9a the shape of a truncated pyramid is observed as it is typical for the MOCVD growth. Symmetrical growth facets can be distinguished. Similar shapes of MOCVD dots were found in [11] and [12] by observation of  $\langle 100 \rangle$  type lattice images.

The shape of MBE grown QDs differs from the shape of those grown by MOCVD. For MBE grown QD samples, the typical shape of the QD is a half-lens. In Fig. 9b a  $\langle 110 \rangle$ -type lattice image of a MBE grown QD is shown. The description of this sample is given in Fig. 5a. The QD shown in Fig. 9b was grown directly on GaAs and was capped by a 5 nm thick  $\text{In}_{0.15}\text{GaAs}_{0.85}\text{As}$  layer.

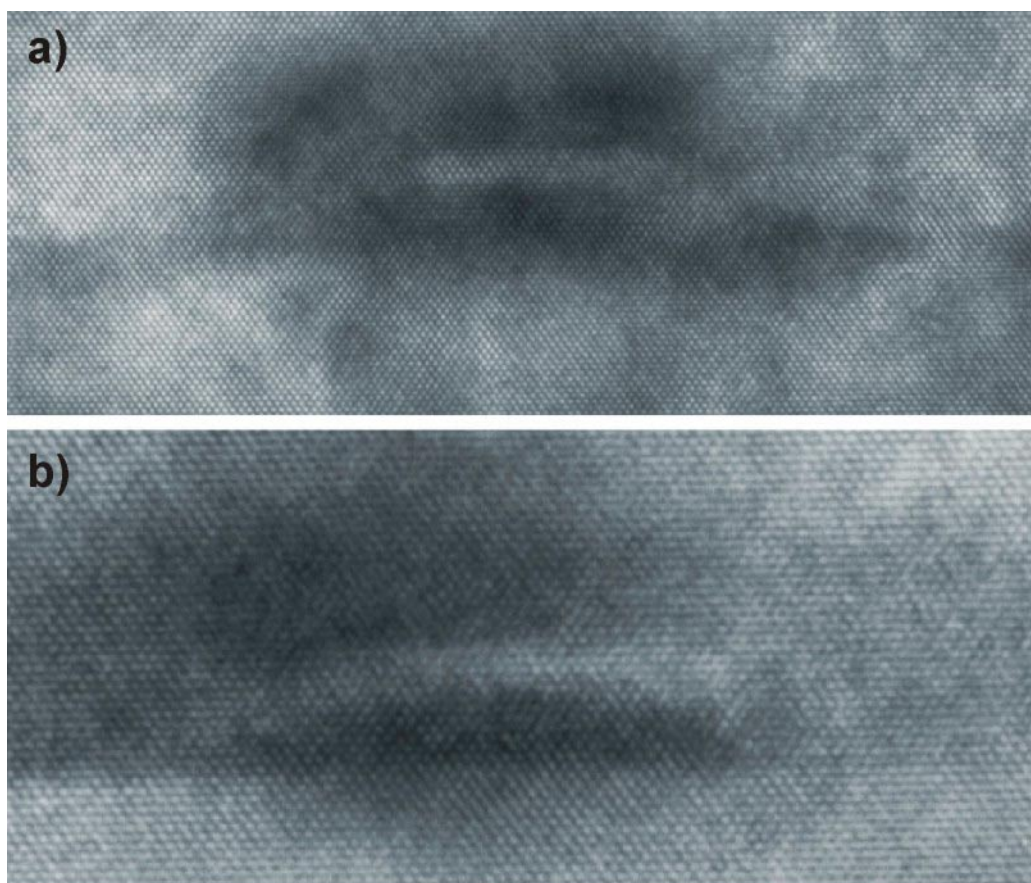


Fig. 9.  $\langle 110 \rangle$  type lattice images of QDs grown by: a) MOCVD and b) MBE. [7]

## Acknowledgment

This publication is based on the work partly sponsored by: the Polish Government under the project #8T11B.064.19, the European Commission under the project “*Gallium Arsenide Second Window Quantum-Dot Lasers*” (IST-1999-10450 GSQ) as well as by the Swiss National Science Foundation and the Polish Government. HRTEM studies were carried out due to the co-operation project between the IET and the MPI-MF according to executive protocols to inter-government agreements signed with the governments of Poland and Germany.

The author is very much indebted to J. Ratajczak, J. Łaszcz, F. Phillipp, M. Bugajski, K. Regiński, J. Muszalski, A. Fiore, C. Paranthoen, A. Passaseo, R. Cingolani, H. Wrzesińska, M. Górksa, M. Guziewicz and A. Piotrowska, for collaboration in research as well as Ms D Szczepańska and Mr J Gazda for assistance in specimen preparation and Ms J Wiącek for careful preparation of micrographs.

## References

1. C. HENGHUBER, H. OPPOLZER AND S. SCHILD, Siemens Forsch. Entwickl. Ber., 9 (1980) 363.
2. O. GESZTI, L. GOSZTOLA AND L. SEYEFRIED, Thin Solid Films, 136 (1980) L35.
3. J. RATAJCZAK, ITE REPORTS, No 9 (1990) 51
4. J. KĄTCKI, J. RATAJCZAK, A. MALĄG AND M. PISKORSKI, Microscopy of Semiconducting Materials 1995 (A.G. Cullis and A.E. Statton Bevan, ed.), IOP, Bristol 1995, p. 273.
5. KĄTCKI J., RATAJCZAK J., PHILLIPP F., MUSZALSKI J., BUGAJSKI M., CHEN J.X., FIORE A.: Electron Microscopy Study of Advanced Heterostructures for Optoelectronics. Materials Chemistry and Physics 2003 vol.81 no 2-3 p. 244.

6. KĄTCKI J., ŁASZCZ A., RATAJCZAK J., PHILLIPP F., GUZIEWICZ M., PIOTROWSKA A.: Transmission Electron Microscopy Study of Au/ZrB<sub>2</sub>/Ag(Te) Contacts to GaSb. *Materials Chemistry and Physics* 2003 vol.81 no 2-3 pp.260.
7. KĄTCKI J., RATAJCZAK J., ŁASZCZ A., PHILLIPP F., FIORE A., PARANTHOEN C., CHEN J.X., PASSASEO A., CINGOLANI R.: Transmission electron microscopy of In(Ga)As QDs heterostructures, *Electron Technology Internet Journal*, 35, 4, 1-7 (2003); <http://www.ite.waw.pl/etij/pdf/35-04p.pdf>.
8. A. PASSASEO, R. RINALDI, M. LONGO, S. ANTONACI, A. L. CONVERTINO, R. CINGOLANI, A. TAURINO, M. CA-TALANO, *Structural Study of InGaAs/GaAs Quantum Dots Grown by Metalorganic Chemical Vapor Deposition for Optoelectronic Applications at 1.3 Micrometers*, *J. Appl. Phys.*, 2001, **89**, 4341–4348.
9. M. DE GIORGI, A. PASSASEO, R. RINALDI, T. JOHAL, R. CINGOLANI, A. TAURINO, M. CATALANO, P. CROZIER, *Nanoscale Compositional Fluctuations in Single InGaAs/ GaAs Quantum Dots*, *phys. stat. sol. (b)*, 2001, 224, 17–20.